PHYSICAL REVIEW B VOLUME 17, NUMBER 6 15 MARCH 1978

Symmetry-related polarization effects in angle-resolved synchrotron photoemission from W(001) and W(001) + H

J. Anderson, G. J. Lapeyre, and R. J. Smith
Montana State University, Bozeman, Montana 59715
(Received 30 September 1977)

We report results of synchrotron photoemission experiments from W(001) and W(001) plus a saturated layer of hydrogen. For *s* polarization, photoemission features are observed whose amplitude depends strongly on the direction of the vector potential $\vec{A}$ with respect to symmetry elements (mirror planes) of the substrate crystral. The observations are explained in terms of selection rules governing transitions between states of specific parity with respect to reflection in the mirror plane. The observations are consistent with the known parities of the tungsten bands and are used to infer parities for the hydrogen-induced states. The observed parities for the hydrogen states place constraints on possible chemisorption models, and support an existing model which specifies two hydrogen atoms per unit mesh in an antisymmetric combination of 1*s* orbitals.

INTRODUCTION

Polarization-dependent angle-resolved uv photoemission spectroscopy (PARUPS) has become an increasingly important technique for the study of the electronic structure of solids, surfaces, and chemisorbed layers.[1,2] The first experiments of this kind were the pioneering work of Gobeli, Allen, and Kane[3] (GAK), reported in 1964. Their purpose was to verify that a significant fraction of photoexcited electrons are emitted from the surface without scattering and consequent loss of information concerning the initial- and final-state wave vector of the observed transitions. In analyzing their data they considered a picture involving direct interband transitions followed by emission wherein $\vec{k}_{\parallel}$, the component of the wave vector $\vec{k}$ parallel to the surface, is conserved. They then used the symmetry properties (parity with respect to a reflection plane in the sample) of the initial- and final-state wave functions $|i\rangle$ and $|f\rangle$ and of the operator $\vec{A}\cdot\nabla$ to determine the vanishing or nonvanishing of the optical matrix elements. They showed that only in the absence of scattering the photocurrent should bear a strong dependence on the direction of $\vec{A}$ in the surface, and they observed this dependence experimentally. Their general formulation of the problem has been exploited in recent investigations of photoemission from Cu and Ag,[4,5] and of GaAs.[2,6]

As summarized in previous articles,[1,2,7] it is possible to turn the argument of GAK around and, from the polarization dependence of prominent transitions observed in photoemission spectra, draw conclusions concerning the symmetry of the wave functions. The purpose of this paper is to present results of PARUPS experiments for the (001) surface of tungsten, both clean and with a saturated layer of chemisorbed hydrogen.

For clean tungsten, the band parities inferred from the polarization dependence agree with calculations, which gives us confidence that the method of analysis is sound and can be applied to other systems. For tungsten plus hydrogen, the relative parities of the initial and final state can be determined from the experimental data. In determining absolute parity, we refer to two different results which are mutually consistent. First, from the photon-energy dependence of the transitions it appears that the tungsten and the hydrogen transitions share common final states. Since the parity of those final states are known, the initial-state parity of the hydrogen transition may be determined. Second, it can be shown from general arguments[8] that only even final states can be observed in the photoemission spectroscopy. This result seems to be borne out experimentally, consequently the hydrogen initial-state parity may be determined.

EXPERIMENTAL

The tungsten sample was a thin ribbon whose surface was within about one degree of the (001) plane. Standard cleaning methods were used and the background pressure was $\approx 1\times 10^{-10}$ Torr. Synchrotron radiation from the storage ring at the University of Wisconsin Synchrotron Radiation Center was focussed to a small spot on the surface at an angle of incidence of 42.3°. Most of the data presented here are for photon energies $h\nu$ between 13 and 20 eV. Using the theoretical polarization of synchrotron radiation and optical properties of surfaces in the optical system the polarization purity is estimated to be 88%.

The photocurrent was detected with a cylindrical mirror analyzer (CMA) modified[9] with an aperture to select a small portion of the emission hemi-

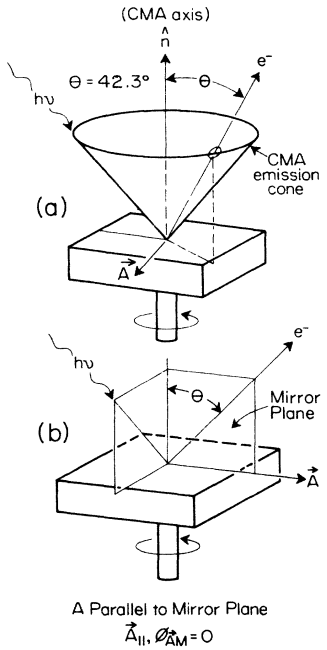

FIG. 1. Experimental geometry. The direction of the detected photocurrent e^- is defined by the moveable 4° circular aperture on the CMA cone. In these experiments the polar angle is fixed at 42.3°. $\vec{A}$ is fixed in space and lies parallel to the surface. Simultaneous rotation of the crystal and the aperture keeps the emission direction fixed relative to the crystal geometry, while rotating $\vec{A}$ in the surface.

sphere. The geometrical arrangement, which is depicted in Fig. 1 can be understood from the following: without the aperture, the CMA passes those electrons whose trajectories lie within ±6° of an acceptance cone, of half angle 42.3°, whose axis coincides with the CMA axis and whose vertex is at the point of illumination (target point). Disregarding mechanical details, the aperture may be considered as a circular hole at the lip of the cone whose diameter subtends four degrees as viewed from the target point. In the experiments we describe, the crystal normal and the CMA axis coincide; therefore, the collection angle was at a constant polar angle θ of 42.3°, while the azimuthal angle could be varied at will by moving the aperture about the lip of the cone and/or rotating the crystal about its normal. The crystal orientation with respect to the light beam was such that the polarization vector $\vec{A}$ remained parallel to the surface as the crystal was rotated. Simultaneous rotation of the crystal and the aperture had the effect of rotating $\vec{A}$ in the plane of the crystal while keeping the emission direction fixed with respect to the crystal. In this way it was possible to observe the effect of changing the direction of $\vec{A}$ in the surface while keeping the emission direction fixed.

THEORY

We make the assumption that the polarization dependence we observed is correctly described by the model used by GAK and submit that its successful application constitutes justification for this model. The model rests upon the following result: that the optical matrix element for the transition $\langle f|\vec{A}\cdot\nabla|i\rangle$ is nonzero only if the integrand has a component which is invarient with respect to the symmetry operations of the crystal.[10] Considering initial- and final-state wave vectors $\vec{k}_i$ and $\vec{k}_f$ which lie in a mirror plane (MP) in the Brillouin zone (BZ), the associated Bloch wave functions must be either even or odd under reflection in that MP if the states are nondegenerate and contain no spin-orbit effects. We consider only MP's normal to the surface. This property is defined as "parity." Spin-orbit coupling, as discussed by GAK, can mix states of different parity, resulting in a reduction in the polarization effect. The operator $\vec{A}\cdot\nabla$ is of even parity if $\vec{A}$ is parallel to the MP ($A_{\parallel}$) and odd if $\vec{A}$ is perpendicular to MP ($A_{\perp}$). It follows then that the matrix element will be identically zero (i) for $\vec{A}_{\perp}$ with $|i\rangle$ and $|f\rangle$ of the same parity, and (ii) for $A_{\parallel}$ with $|i\rangle$ and $|f\rangle$ of opposite parity and nonzero otherwise. GAK also showed that for $\vec{A}$ in the surface but at some arbitrary angle $\phi_{\vec{A}M}$ to the MP, the emission varies as $\cos^2\phi_{\vec{A}M}$ or $\sin^2\phi_{\vec{A}M}$, depending on whether $|i\rangle$ and $|f\rangle$ are of the same or opposite parity, respectively. For $\vec{k}_i$ and $\vec{k}_f$ off the MP, the Bloch functions have no definite parity so the emission will in general not vanish for any direction of $\vec{A}$. However, a smaller residual polarization dependence will remain depending on the predominant parity of $|i\rangle$ and $|f\rangle$. This can be seen by expanding $|i\rangle$ and $|f\rangle$ in even and odd basis functions and calculating the matrix element which will contain terms in $\cos^2\phi_{\vec{A}M}$ and $\sin^2\phi_{\vec{A}M}$ as well as cross terms.

An alternative description of the polarization effect exists[11] from which the same results may be derived. By putting explicit series expansions for $|i\rangle$ and $|f\rangle$ into the Fermi golden rule, the authors of Ref. 11 obtain a formula for the angle-dependent transition rate. The result bears little superficial resemblance to the treatment of GAK, however it is not hard to show that when $|i\rangle$ and $|f\rangle$ have even or odd parity, conditions are imposed on the form of the expansions such that the same rules are obtained. The formulation thus contains that of GAK as a special case and has the added advantage that it permits in principle explic-

it calculation of the photocurrent. Also implicit is the remarkable result, derived rigorously by Hermanson,[8] that if one measures emission in a mirror plane, then one cannot observe transitions to odd-parity final states.

It should be noted that within the model of GAK, the orientation of $\vec{A}$ to the emission direction plays no explicit role. Thus, for some hypothetical pair of $|i\rangle$ and $|f\rangle$, where $\vec{k}_i$ and $\vec{k}_f$ lie off the MP yet have a definite parity with respect to it, it is the *orientation of* $\vec{A}$ *to that* MP *alone* that determines the transition rate. The reason that the present experiments were performed measuring the emission in a MP is because then the parity of the states is guaranteed (apart from the possibility of degenerate bands or strong spin-orbit effects).

The polarization effect is observed as a strong modulation in the amplitude of a peak in the photoemission spectra as $\vec{A}$ is rotated between $\vec{A}_\parallel$ and $\vec{A}_\perp$. In cases where the initial- and final-state band assignments can be established by independent means, the sense of the polarization effect (strong for $\vec{A}_\parallel$ and weak for $\vec{A}_\perp$ or vice versa) should be consistent with those assignments. If the band assignments are uncertain then the sense of the polarization dependence might be decisive in establishing them.

Most of the data we present are for the following experimental configuration: the emission plane coincides with the mirror plane so that $\vec{k}$ and $\vec{k}_\parallel$ lie in that plane. The emission amplitude depends on the angle ϕ_{AM} between $\vec{A}$ and the selected MP, and our analysis of the results exploits the invariance of $\vec{k}$ with respect to reflection in the MP. Therefore, in order to display transparently the MP involved in a particular experiment we adopt a notation defined in the following illustrations: if the azimuthal emission angle ϕ is such that the emission lies in the (100) plane, we use as an abbreviated expression "$\phi = (100)$." Alternatively we say that the emission is in the (100) azimuth. Also, "$\vec{k}_\parallel = 1.0$ Å^{-1}, (100), $\vec{A}_\parallel$" means that $\vec{k}_\parallel$ lies in the (100) MP, has a magnitude of 1.0 reciprocal angstrom, and that $\vec{A}$ is parallel to that plane.

EXPERIMENTAL RESULTS

A. Clean tungsten (001)

For emission in the (100) or (110) mirror planes there are a number of peaks in the photoemission spectra, taken at several photon energies, that exhibit a strong polarization dependence. Figure 2 shows a set of two angle-resolved energy-distribution curves (AREDC's) taken at $h\nu = 20$ eV in the (100) MP for $\vec{A}_\parallel$ (upper curve) and $\vec{A}_\perp$ (lower curve) plotted as a function of initial energy E_i below the Fermi energy E_F. There is a predominant peak at $E_i = -5.4$ eV which is strong for $\vec{A}_\parallel$ and weak for $\vec{A}_\perp$. It should be noted that because of the four-fold symmetry of the surface both experimental configurations have $\vec{A}$ in crystallographically equivalent directions and the emission directions in crystallographically equivalent directions. The nonequivalence lies in the direction of $\vec{A}$, with respect to the plane about which $|i\rangle$ and $|f\rangle$ have a specific parity, as discussed above.

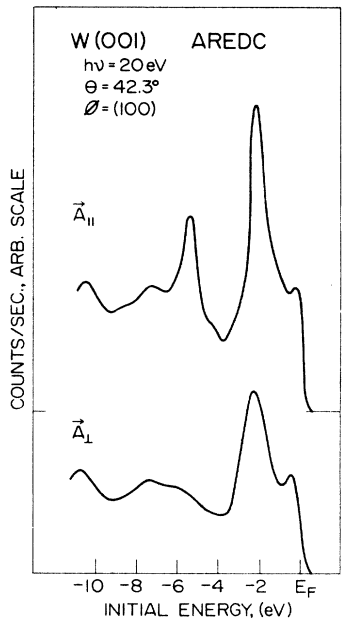

FIG. 2. Angle-resolved EDC for clean tungsten, showing effect of polarization direction on the peak at $E_i = -5.4$ eV. Emission direction is in (100) mirror plane. The direction of $\vec{A}$ is parallel to the MP ($A_\parallel$) and perpendicular to the MP ($A_\perp$).

To identify the initial and final bands involved in the transition we use the tungsten band-structure calculations of Christensen and Feuerbacher.[12] Only the parallel (to the surface) component $\vec{k}_\parallel$ of the wave vector $\vec{k}$ is conserved in the photoemission process while the normal component of the emitted electron's momentum need bear no simple relation to the internal wave vector.[13] For the -5.4-eV peak we find $|k_\parallel| = \sin\phi\,(2mE_k)^{1/2}/\hbar = 1.1$ Å^{-1}, where m is the electron mass and E_k is the kinetic energy of the emitted electron. The condition $\vec{k}_\parallel = \text{const}$ defines a line in the BZ which is normal to the surface and, for direct transitions, the final wave vectors must terminate on this line.

Figure 3 shows the tungsten energy bands along the line $\vec{k}_\parallel = 1.0$ Å^{-1}, (100). This suffices to identify the bands associated with $\vec{k}_i$ and $\vec{k}_f$ for the transition because the bands for $\vec{k}_\parallel = 1.1$ Å^{-1} differ only slightly from those shown. Figure 4 shows the

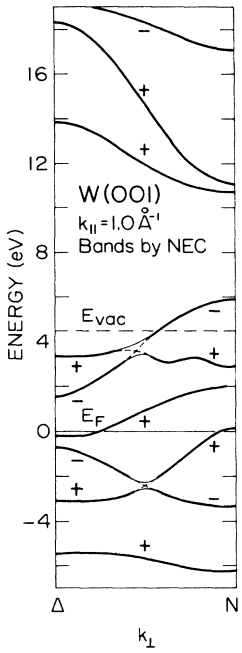

FIG. 3. Tungsten energy bands along a line parallel to the Δ line for $k_{\parallel}=1.0$ Å^{-1}, (100). Bands by N. E. Christensen (Ref. 12).

first BZ indicating the vertical line, labeled (1), along which the bands are plotted. The evident choice for initial and final bands is band 1 for $|i\rangle$ and band 7 for $|f\rangle$ where the bands are numbered in order of increasing energy. The experimental and calculated energies agree very well. The parity assignments are obtained from the nonrelativistic band calculations of Petroff and Viswanathan[14] which should be applicable in regions of the

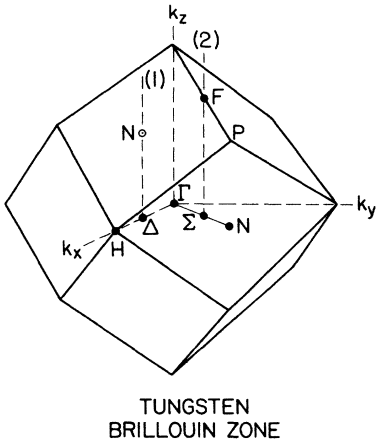

FIG. 4. First Brillouin zone for tungsten (bcc) indicating various symmetry lines and points. The bands in Fig. 3 are plotted along the dashed line (a); those in Fig. 6 are plotted along the dashed line (b).

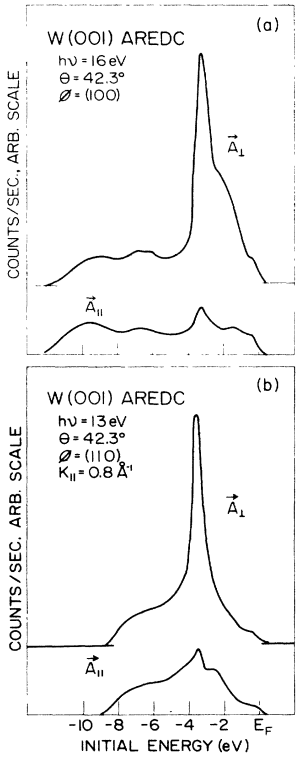

FIG. 5. (a) Clean tungsten emission in the (100) mirror plane for $h\nu=16$ eV. (b) Clean tungsten emission in the (100) mirror plane for $h\nu=16$ eV. (a) and (b). The peak at $E_i=3.3$ eV is large for $A_\perp$ and small for $A_{\parallel}$, showshowing that the initial- and final-state bands have opposite parity.

BZ where there are no appreciable spin-orbit effects.[15] Both band 1 and band 7 have even parity (+), which is consistent with the experimentally observed sense of the polarization effect.

Figure 5(a) shows a set of two AREDC's, taken at $h\nu=16$ eV, with emission in the (100) plane, for $\vec{A}_\perp$ and $\vec{A}_{\parallel}$ with respect to that mirror plane. Figure 5(b) is the same for $h\nu=13$ eV, with emission in the (110) plane. Both figures show a large peak at about the same initial energy: $E_i=3.3$ eV and 3.5 eV, respectively. Both are strong for $\vec{A}_\perp$ and we discuss them in turn. (a) $h\nu=16$ eV. For this peak we have $\vec{k}_{\parallel}=1.0$ Å^{-1} (100) so that Fig. 3 shows the correct energy bands. Only the second band has the correct E_i, while only bands 7 and 8 span the region of the observed final-state energy $E_f=12.7$ eV. The sense of the polarization dependence requires opposite parity for $|i\rangle$ and $|f\rangle$ and since both bands 7 and 8 are even, we are led to locate the transition on the right-hand portion of the band diagram, where band 2 is odd. It might be expected that the transition is strongest near N in the zone, where the bands are flat and parallel, but experimentally the largest amplitude occurs at

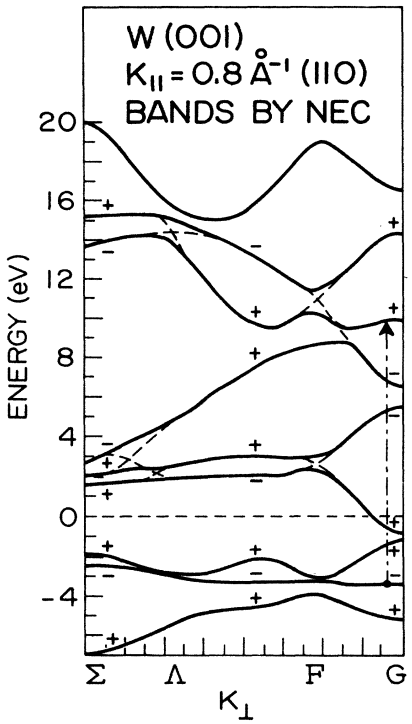

FIG. 6. Tungsten energy bands along the line parallel to the Δ line for $\vec{k}_{\parallel} = 0.8$ Å^{-1} in the (110) azimuth.

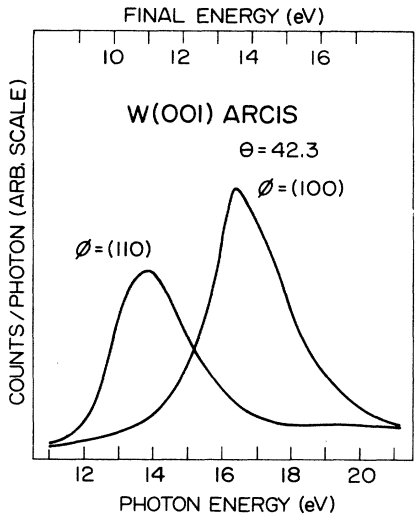

FIG. 7. Angle-resolved CIS's for tungsten with $E_i = -3.3$ eV and azimuthal angle corresponding to the initial-state peaks shown in Fig. 5.

$E_f = 13$ eV which is about 2 eV too high. (b) The $h\nu = 13$ eV peak. In this case $\vec{k}_{\parallel} = 0.8$ Å^{-1}, (110), and Fig. 6 shows the relevant bands plotted along the vertical line labeled (2) in Fig. 4. Again band 2 appears to be the correct initial-state band. In fact the second band is fairly constant in energy over a large region of the zone between $\vec{k}_{\parallel} = 0.8$ Å^{-1}, (100), and $\vec{k}_{\parallel} = 0.8$ Å^{-1}, (110), which accounts for the frequent occurrence of a peak near this initial energy in tungsten photoemission experiments. From Fig. 6 band 7 appears to be the most likely final-state band, its energy and parity being consistent with the experimental observations.

The two latter photoemission peaks evidently correspond to transitions from a fairly flat band 2 to final bands in different regions of the BZ at which there occurs a large joint density of states for $h\nu = 13$ and 16 eV, respectively. Since E_i is fairly constant with $h\nu$, it is possible to measure the peak amplitude (plus background) continuously as a function of $h\nu$ by the constant initial-energy spectrum (CIS) method.[1] The method consists of sweeping the analyzer energy window and $h\nu$ simultaneously while maintaining $h\nu - E_f$ constant and equal to the desired E_i, corresponding to the peak position. One is in effect measuring the peak height over a continuous range of EDC's and can observe the transition amplitude over the corresponding range of final-state energies. Figure 7 shows two such angle-resolved CIS's for the two emission peaks under discussion. The straightforward interpretation is that transition from band 2 "finds" large joint densities of states at $E_f = 10.5$ eV for $\vec{k}_{\parallel} = 0.8$ Å^{-1}, (110), and $E_f = 13$ eV for $\vec{k}_{\parallel} = 1.0$ Å^{-1}, (100), respectively. This is essentially a reiteration of the information contained in the EDC's, except from the EDC's alone it is not clear that the transitions are at or near the maximum amplitude.

Another perspective on the emission properties of these peaks can be obtained in the following experiment. The CMA aperture was held at a constant position so as to make A perpendicular to the emission plane, the photon energy was held fixed and the sample was rotated about its normal while measuring the emission current. The resulting polar plot of emission versus crystal rotation angle we call a "crystal ϕ pattern" and it is shown for $h\nu = 13.5$ eV, $h\nu = 15$ eV, and $h\nu = 16$ eV in Fig. 8. The crystal orientation is indicated by the angular positions of the important (100) and (110) planes. For $h\nu = 13.5$ eV, $\phi = (110)$ and $h\nu = 16$ eV, $\phi = (100)$ we recover the conditions for maximum peak amplitude. The $h\nu = 15$ eV curve is an inbetween case. The variation in emission at intermediate angles is due to several effects which would be difficult to separate. They are (i) the detailed behavior of the bands at the corresponding regions of the BZ; (ii) the mixed parity of the initial and final states; and (iii) the variation of the angle $\phi_{\vec{A}M}$ between A and the mirror planes. The curves give the appearance of a "rotation" of the major lobes from

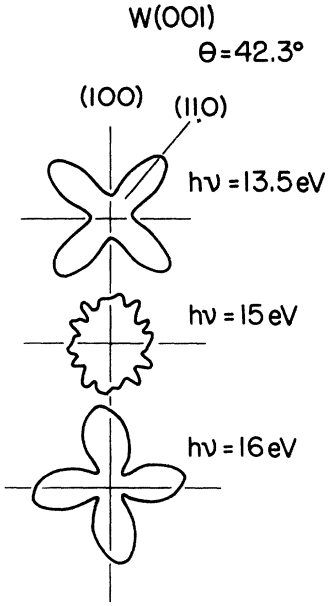

FIG. 8. "Crystal ϕ patterns" for the polarization-dependent peaks in Fig. 5. These were obtained by rotating the crystal and holding $E_i, h\nu$ direction of $\vec{A}$, and emission direction fixed, as explained in the text.

one azimuth to the other, but of course they really only manifest the emission properties elucidated above.

For the emission peak of $h\nu = 13$ eV, we have determined that $|i\rangle$ and $|f\rangle$ are of opposite parity with respect to reflection in the (110) MP. We expect, then, that the emission amplitude would vary as $\sin^2\phi_{\vec{A}M}$. Figure 9 shows a plot of peak height above the background as a function of $\phi_{\vec{A}M}$. Except for the fact that the emission does not entirely vanish for $\phi_{\vec{A}M}=0$, we obtain the correct angular dependence to a satisfactory degree of

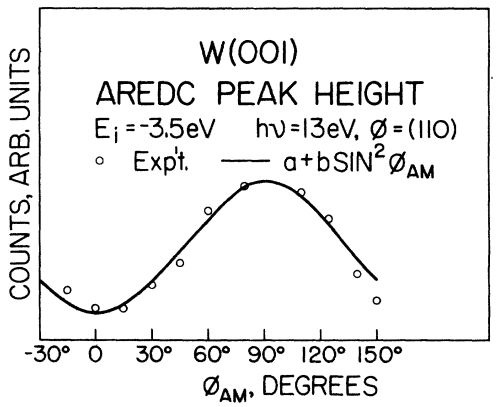

FIG. 9. Amplitude of polarization-dependent peak in Fig. 5(b) as a function of the angle ϕ_{AM} between $\vec{A}$ and the (110) mirror plane.

accuracy.

The tungsten data we have presented provides an overall consistent picture of the behavior of the photoemission peaks observable with our experimental configuration and which exhibit the polarization effect. Except for the -3.3-eV peak [Fig. 5(a)], for which the measured final-state energy is somewhat higher than expected, the data agree in detail with the calculated energies and parities of the tungsten energy bonds. As a result, we believe it is justified to apply the same sort of analysis to other photoemission systems.

B. W(001) + H_2 saturated

Having analyzed the polarization dependence of some tungsten emission peaks in terms of band parity, it is possible to do the same for prominent emission peaks that appear as a result of saturated adsorption of hydrogen. A monolayer is defined as saturated adsorption even though it is generally believed that there are two H atoms for one W surface atom. Our analysis rests on certain observations and premises. First, many of the chemisorption peaks exhibit a polarization dependence similar to that observed for the clean tungsten. This fact does not of itself imply that the hydrogen-induced initial states are bandlike, since the symmetry arguments hold both for localized orbitals and for bandlike states. However there is ample evidence that the hydrogen states do form bands, and the two-dimensional band structure corresponding to many of the prominent photoemission features has been determined experimentally.[16] Therefore, we refer to the initial states manifested in the photoemission spectra as hydrogen bands, and the analysis of the polarization dependence proceeds as in the clean tungsten case. The circumstance that the hydrogen bands are two dimensional should introduce no ambiguity with respect to defining a parity with respect to reflection in a three-dimensional mirror plane, since the MP's are normal to the surface and the reflection operation $x \rightarrow -x$ is the same irrespective of the reduced dimensionality of the relevant bands. Second, it is necessary to know the parity of the final state in order to determine the parity of the hydrogen initial-state band. From the discussion in Sec. III we know that for photoemission in a mirror plane only even final states may be observed, so that the initial-state parity may be inferred directly from the sense of the polarization dependence. This result seems to be borne out experimentally in the data we have shown: all the final-state bands are evidently of even parity. It should be observed, however, that the portions of those bands (7 and 8) which span the range of

final-state energies in these experiments are mostly even throughout. Sufficiently detailed and comprehensive experiments to determine whether odd final states can or cannot be identified have not yet been done.

For the case of chemisorbed hydrogen we can determine the absolute parity of the hydrogen bands from the sense of the polarization effect and the requirement of even final states. An independent check on the parity assignments could be made if the parities of the final states were known. Such knowledge may, in fact, be available from an analysis of the hydrogen on tungsten data: we present evidence that the final-state bands for the hydrogen-induced transitions are the same as for the tungsten transitions, with the parities of those bands already determined as discussed above.

Figure 10 shows four AREDC's, taken at $h\nu = 20$ eV, emission in the (100) plane for the four combinations of W, W+H, and $\vec{A}_{\parallel}$, $\vec{A}_{\perp}$. The clean tungsten curves are the same as in Fig. 2. The hydrogen induced doublet within 2 eV of E_F does not show much polarization dependence, but the hydrogen peak at $E_i = -6.5$ eV does.[17] For this latter peak we have $\vec{k}_{\parallel} = 1.0$ Å^{-1}, (100), strong for $\vec{A}_{\parallel}$. The coincidence of these final-state parameters with those for the −3.3-eV peak in Fig. 5(a) is shown in Fig. 11 which displays CIS's of the

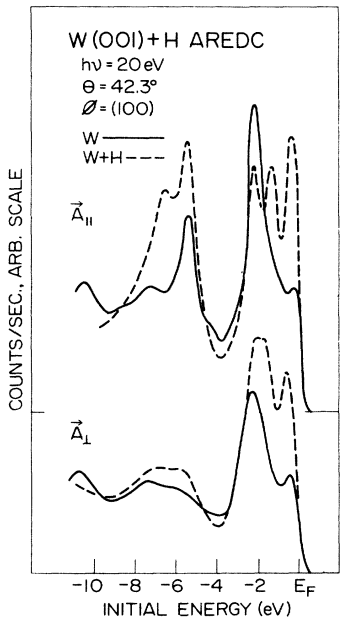

FIG. 10. Angle-resolved EDC's for tungsten and tungsten plus hydrogen for the $\vec{A}_{\perp}$ and $\vec{A}_{\parallel}$ configurations, showing the polarization dependence of the hydrogen peak at $E_i = -6.5$ eV. The clean tungsten curves are the same as in Fig. 2.

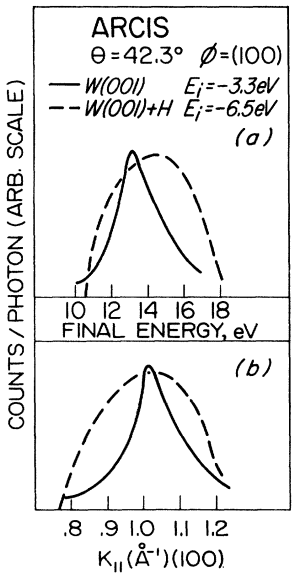

FIG. 11. Angle-resolved CIS's for (a) the tungsten peak at $E_i = -3.3$ eV, solid line, and (b) the hydrogen peak at $E_i = -6.5$ eV, dashed line. This figure illustrates the coincidence of the final-state parameters for the two transitions.

peaks plotted against E_f [Figure 11(a)] and $|k_{\parallel}|$ [Figure 11(b)]. For the hydrogen peak we have plotted the enhancement divided by the tungsten background emission. Although the hydrogen curve is rather broader than the tungsten, the two curves have their maxima at the same $|k_{\parallel}|$, 1.0 Å^{-1} (the

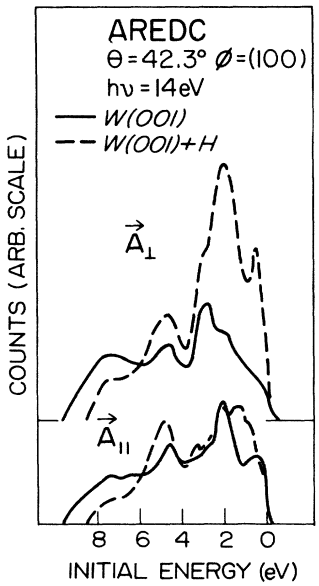

FIG. 12. Angle-resolved EDC's, similar to those of Fig. 10 but with the experimental parameters as indicated. The curves show the polarization-dependent hydrogen peaks at $E_i = -0.5$ eV and $= -2$ eV.

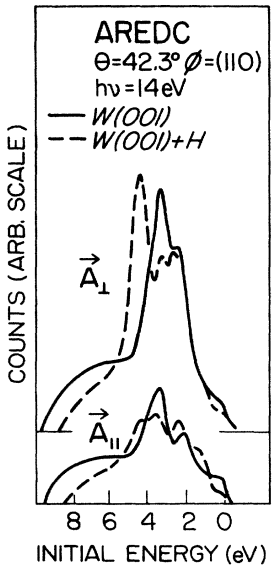

FIG. 13. Curves similar to those of Fig. 12 but with experimental parameters as indicated. The polarization-dependent hydrogen peak is at $E_i = -4.3$ eV.

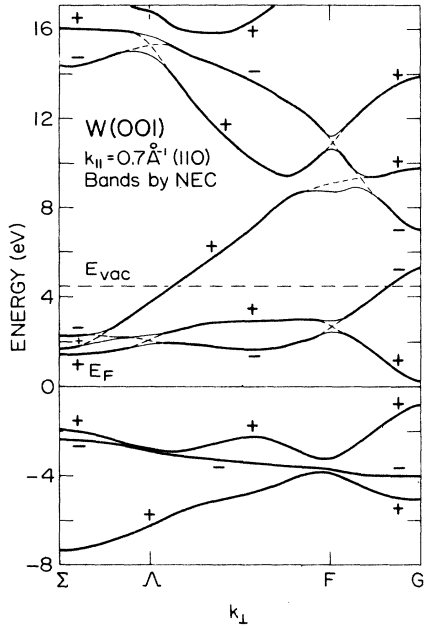

FIG. 14. Tungsten energy bands for the line in the BZ parallel to the Δ line for $\vec{k}_{\parallel} = 0.7$ Å^{-1} in the (110) azimuth.

slight shift in the coincidence in E_f reflects the work function difference for the two cases). From this evidence, we suggest the assignment of either band 7 or 8 as the final band for the hydrogen emission peaks.

Figure 12 shows four more AREDC's in the manner of Fig. 10 but taken at $h\nu = 14$ eV, (100) emission plane. The narrow hydrogen peak at $E_i = -0.5$ eV and the broader one at $E_i = -2$ eV correspond to transitions with $|k_{\parallel}| = 1.0$ Å^{-1} and 0.9 Å^{-1}, respectively. The H peaks in Fig. 12 show the opposite polarization dependence to those observed in Fig. 10. If we again identify the final band as band 7 or 8, then in this case the sense of the polarization effect implies odd parity for these hydrogen bands. It is interesting to note that the somewhat similar hydrogen peaks near E_f shown in Fig. 10 show little dependence on the direction of $\vec{A}$.

A final example for which we have taken systematic data is the hydrogen peak at $E_i = -4.3$ eV shown in Fig. 13. In this case we have $E_f = 9.7$ eV, $\vec{k}_{\parallel} = 0.71$ Å^{-1}, (110), with emission strong for $\vec{A}_{\perp}$. We identify the final-state band as band 7 from the diagram in Fig. 14 and thereby infer odd parity for this hydrogen band.

The observations described above are summarized in Table I.

DISCUSSION

We have found a strong polarization dependence for photoemission peaks for the systems W (001) and W (001) + H and have interpreted this dependence in terms of the parities of the initial and final states. Tungsten was a good case for testing whether the ideas and methods we have used really work or not because extensive band structure calculations exist which have been shown to be rea-

TABLE I. Experimental observations for W(001) and W(001) + H.

System	Initial-state and energy		Final-state and energy		Mirror plane	Initial-state parity
W	Band 1	−5.4 eV	Band 7	14.6 eV	(100)	even
W	Band 2	−3.3 eV	Band 7	12.7 eV	(100)	odd
W	Band 2	−3.5 eV	Band 7	9.5 eV	(110)	odd
W+H	H,	−6.5 eV	Band 7 or 8	13.5 eV	(100)	even
W+H	H,	−4.3 eV	Band 7	9.7 eV	(110)	odd
W+H	H,	−0.5 eV	Band 7 or 8	13.5 eV	(100)	odd
W+H	H,	−2.0 eV	Band 7 or 8	12.0 eV	(100)	odd

sonably accurate.[18]

Both for cases like tungsten, where the overall accuracy of the band calculations might be conceded, and for other systems whose electronic structure is less understood, exploitation of the polarization dependence confers several significant benefits. One of these is the obvious possibility of obtaining information about wave-function symmetry in addition to energy and wave-vector properties as in ordinary angle-resolved photoemission. From a practical point of view, the experimenter is able to distinguish between and separate, degenerate or close-lying bands, if they have opposite parity, by choosing the appropriate experimental geometry. This method has been used by us with good success in our studies of the band structure of Ni.[19] In studying the chemisorption of CO on Ni we have been able to "tune out" a large, interfering Ni peak in order to study the behavior of a smaller CO peak occurring about 2 eV ϕ below the Fermi level.[20]

In addition to the study of bulk properties, the systematic use of polarization effects in photoemission should be of considerable utility in investigating clean and chemisorbed surfaces. A determination of the parities of the electron wave functions involved in the chemisorption band clearly imposes constraints on the various physical and theoretical models that may be proposed.

For the case of hydrogen on tungsten, few theories specifically address the question of wave-function symmetry. Anders *et al.*[21] invoke the total symmetry of the H 1*s* orbital to specify those combinations of tungsten 5*d* orbitals that can mix with it. Gadzuk[22] likewise constructs initial wave functions from the W-5*d*'s and H-1*s*. Both theories treat an isolated hydrogen atom on a tungsten surface and it would appear that neither can be carried over to the case of full coverage. Any acceptable model must account for the existence of odd-parity states. For an isolated hydrogen atom or even for one per unit mesh this does not appear to be possible, at least within a LCAO picture, because of the intrinsic spherical symmetry of the 1*s* orbital and the requirement that the Bloch functions be periodic in the lattice. It does not seem reasonable to include the H 2*p* orbitals since they lie some 10 eV higher in energy.

A possible resolution of the problem lies in the recent work of Smith and Mattheiss.[23] They calculated the electronic structure of a slab of tungsten atoms and a sheet of hydrogen atoms separately and in union. They make the assumption, for which there is some experimental evidence, that there are two H atoms per unit mesh in bridge sites. Their calculations give the remarkable result that for the hydrogen sheet, the lowest energy configuration is for the *antisymmetric* combination of H 1*s* in the unit mesh. With this picture it is easy to account for an odd-parity initial state. Figure 15 shows their model of the hydrogen saturated W (001) surface and depicts the W 5 $d_{x^2-y^2}$ and H 1*s* orbitals with the phases of the latter in the antisymmetric configuration given by plus and minus signs. This combination gives rise to an energy band (the lowest in their diagram) for the combined W+H system and it clearly has odd parity about the (110) plane. We identify that band with two of the photoemission peaks we observed for W+H (Figs. 9 and 12) and there are several points of agreement which make this identification plausible. The initial state corresponding to the hydrogen peak in Fig. 12 agrees with the calculated band of Smith and Mattheiss in energy $\vec{k}_{\parallel}$ and parity [odd about (110)]. The same band is even about (100) and its energy at $\vec{k}_{\parallel} = 1.0$ Å^{-1}, (100)—i.e., at $\bar{X}$ in the surface zone, is calculated to be −3.4 eV. We find at that $k_{\parallel}$ (Fig. 9) the parity correct but the energy about 3 eV lower than calculated. Smith and Mattheiss note a similar discrepancy between their calculations and the experimental results of Feuerbacher and Willis and stipulate the preliminary nature of their results owing to the sensitive dependence of those results to the choice of LCAO parameters. Nevertheless their model (more specifically, its essential feature—the antisymmetric H 1*s* combination) is the only one we know of which appears to have the capability of explaining our results. In this connection it must be noted that one of our parity as-

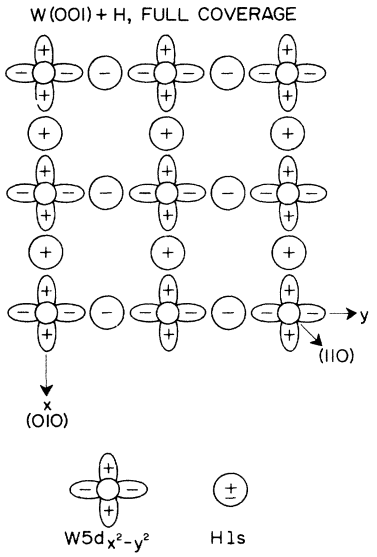

FIG. 15. Hydrogen chemisorption model of Smith and Matheiss. The phases of the tungsten and hydrogen orbitals are indicated by the plus and minus signs.

signments cannot be explained on the basis of the model we have been using. The hydrogen peaks (the doublet in Fig. 11) correspond to initial states with odd parity about the (100) plane. By the same reasoning used earlier, such a symmetry does not seem possible on this model. We hope this example does not constitute a fatal flaw in our analysis, but at present we do not know. In any event, the experimental results are unambiguous and must be dealt with in any theory of chemisorption.

We have presented results for those photoemission features accessible to our experimental configuration. There are, for the tungsten and tungsten-hydrogen system other photoemission features whose behavior might be explainable in terms of such symmetry arguments. For instance, Feuerbacher and Fitton[24] have found normal emission peaks which are strong for p but weak for s polarization. They interpret this observation in terms of various theories for the surface photoelectric effect.[25,26] However, as discussed by Hermanson,[8] their results may be simply a manifestation of a possible Δ_1 symmetry of the initial states.

Symmetry considerations of the type described here have, in the past, been little used in the execution and analysis of photoemission experiments. However, we believe our present results represent a worthwhile advance in understanding the chemisorption of hydrogen on tungsten as well as demonstrating an important aspect of the investigative power of polarization-dependent–angle-resolved synchrotron photoemission. The application of these techniques to other clean and chemisorbed surfaces should be of considerable value in the understanding of those systems as well. The case of a chemisorption orbital with cylindrical symmetry about the surface normal, i.e., CO on nickel, is a case in point. The emission azimuth defines a mirror plane about which the orbital, by definition, and the final-state plane wave have even parity. The rule concerning $A_\perp$ and $A_\parallel$ should apply, and such effects have in fact been observed for emission from the 4σ orbital of CO adsorbed on Ni(001).[27]

ACKNOWLEDGMENT

This research was supported by AFOSR under Grant No. 75-2872. The Wisconsin Radiation Center was supported by NSF under Grant No. 144-F805. The cooperation of E. Rowe, R. Otto, and the UWSRC staff is deeply appreciated.

[1]G. J. Lapeyre, R. J. Smith, and J. Anderson, J. Vac. Sci. Technol. 14, 384 (1977).
[2]G. J. Lapeyre and J. A. Knapp, Nuovo Cimento (to be published).
[3]G. W. Gobeli, F. G. Allen, and E. O. Kane, Phys. Rev. Lett. 12, 94 (1964).
[4]H. Becker, E. Dietz, U. Gerhardt, and H. Angemuller, Phys. Rev. B 12, 2084 (1975).
[5]E. Dietz, H. Becker, and U. Gerhardt, Phys. Rev. Lett. 36, 1397 (1976).
[6]J. A. Knapp, Ph.D. thesis (Montana State University, 1976) (unpublished).
[7]G. J. Lapeyre, J. Anderson, and R. J. Smith, Photoemission from Surfaces, in Proceedings of International Conference, Noordwijk, Holland, Sept., 1976 (unpublished).
[8]J. Hermanson, Solid State Commun. 22, 9 (1977).
[9]J. A. Knapp, G. J. Lapeyre, N. V. Smith, and M. M. Traum (unpublished).
[10]L. M. Falicov, *Group Theory and its Physical Applications* (University of Chicago, Chicago, 1966), p. 118.
[11]N. V. Smith, M. M. Traum, J. A. Knapp, J. Anderson, and G. J. Lapeyre, Phys. Rev. B 13, 4462 (1976). A more detailed derivation of this formulation will be published by M. M. Traum.
[12]N. E. Christensen and B. Feuerbacher, Phys. Rev. B 10, 2349 (1974).
[13]In some experimental situations there seems to be some remnant of $k_\perp$ conservation. See, for example, G. J. Lapeyre *et al.*, Proceedings of the Transition Metal Physics Conference, Toronto, 1977 (unpublished), and references therein.
[14]I. Petroff and C. R. Viswanathan, Phys. Rev. B 4, 799 (1971).
[15]Spin-orbit interaction breaks the mirror plane symmetry, resulting in no exact parity for the Bloch states.
[16]B. Feuerbacher and R. F. Willis, Phys. Rev. Lett. 36, 1339 (1976).
[17]The enhancement of the −6-eV peak in Fig. 9 is not due to a new chemisorption state but probably arises as a consequence of the change in work function when hydrogen chemisorbs.
[18]R. J. Smith, J. Anderson, J. Hermanson, and G. J. Lapeyre, Solid State Commun. 19, 975 (1976).
[19]R. J. Smith, J. Anderson, J. Hermanson, and G. J. Lapeyre, Solid State Commun. 21, 459 (1977).
[20]R. J. Smith, J. Anderson, and G. J. Lapeyre, Bull. Am. Phys. Soc. 22, 413 (1977).
[21]L. W. Anders, R. S. Hansen, and L. S. Bartell, J. Chem. Phys. 59, 5277 (1973).
[22]J. W. Gadzuk, Surf. Sci. 43, 44 (1973); Phys. Rev. B 10, 5030 (1974).
[23]N. V. Smith and L. F. Mattheiss, Phys. Rev. Lett. 37, 1494 (1976).
[24]B. Feuerbacher and B. Fitton, Solid State Commun. 15, 301 (1974).
[25]G. D. Mahan, Phys. Rev. B 2, 4334 (1970).
[26]J. G. Endriz, Phys. Rev. B 7, 3463 (1973).
[27]R. J. Smith, J. Anderson, and G. J. Lapeyre, Phys. Rev. Lett. 37, 1081 (1976).